Multiple new site-specific recombinases for use in manipulating animal genomes

Aljoscha Nern[1], Barret D. Pfeiffer[1], Karel Svoboda, and Gerald M. Rubin[2]

Janelia Farm Research Campus, Howard Hughes Medical Institute, Ashburn, VA 20147-2408

Contributed by Gerald M. Rubin, July 18, 2011 (sent for review June 22, 2011)

Site-specific recombinases have been used for two decades to manipulate the structure of animal genomes in highly predictable ways and have become major research tools. However, the small number of recombinases demonstrated to have distinct specificities, low toxicity, and sufficient activity to drive reactions to completion in animals has been a limitation. In this report we show that four recombinases derived from yeast—KD, B2, B3, and R—are highly active and nontoxic in *Drosophila* and that KD, B2, B3, and the widely used FLP recombinase have distinct target specificities. We also show that the KD and B3 recombinases are active in mice.

gene expression | genetic engineering

Site-specific DNA recombinases are widely used in multicellular organisms to manipulate the structure of genomes and, in turn, to control gene expression (for reviews see refs. 1–4). These enzymes, derived from bacteria and fungi, catalyze directionally sensitive DNA exchange reactions between short (30–40 nucleotides) target site sequences that are specific to each recombinase (5). These reactions enable four basic functional modules—excision/insertion, inversion, translocation and cassette exchange—that have been used individually or combined in a wide range of configurations to control gene expression (Fig. 1*A*).

The use of site-specific recombination to manipulate genomes has been limited by the availability of recombinases with high activity, distinct site specificity, and low toxicity. In *Drosophila*, the most widely used recombinase is FLP, encoded by the *Saccharomyces cerevisiae* 2-μm plasmid (6). FLP was first shown to work in a heterologous, multicellular organism by Golic and Lindquist in 1989 (7) who demonstrated the excision reaction on chromosomally inserted target sites (FRTs). Since that time FLP/FRT recombination has been widely used in *Drosophila* in applications based on excision (8) and translocation (9–11).

Complex manipulations of genome structure can require the use of more than one of the modules diagrammed in Fig. 1*A*, or parallel independent implementations of the same module, in a single individual. To accomplish such manipulations, the modules must be implemented with different recombinases that do not recognize each other's target sites. Similarly, a number of powerful methods have been developed for using the excision and inversion reactions to control expression of a transgene specifically in cells where two independent gene expression patterns overlap (2, 3, 12, 13). Such intersectional methods rely on pairs of orthogonal recombinases; see, for example, Fig. 1*B*. For these reasons, we sought to discover additional recombinases with distinct site-specificity.

FLP recombinase has been mutated to recognize altered FRT sites, but some cross-reaction still remains (14, 15). Cre, encoded by the bacteriophage P1, is the most widely used recombinase in mammalian cells (16–18). Cre functions in *Drosophila* (19), but exhibits obvious toxicity (20), a problem also observed in mammalian cells (21, 22; reviewed in ref. 23) and plants (24).

Other site-specific recombinases have been used in metazoans, but less extensively. Dre recombinase, a close relative of Cre, has been demonstrated to work in mammalian cells (25, 26). PhiC31 integrase, which catalyzes unidirectional recombination between *attP* and *attB* sequences, has been used extensively for integration (27, 28) and cassette exchange (29, 30), applications that take advantage of its nonreversibility. The R recombinase, a relative of FLP from the yeast *Zygosaccharomyces rouxii* (31, 32), has been shown to function in plants (33).

In this report we describe the characterization of R and three other recombinases encoded by 2-μm circle-like plasmids of other yeasts. Although such plasmids are rare among yeasts, those characterized so far are very similar in structure to the 2-μm plasmid of *S. cerevisiae* (reviewed in ref. 34). In particular, they appear to encode site-specific recombinases related to FLP and undergo high-frequency intramolecular recombination between inverted repeat domains both in their native species and in *S. cerevisiae* (32, 34–39). However, only the R recombinase has previously been shown to work in a multicellular organism (33), and none has been used in an animal genome. We compare the properties of these four yeast recombinases to FLP, Cre, and Dre in *Drosophila*. We demonstrate four non–cross-reacting pairs of recombinases and target sites that have low toxicity and high activity. We also show that two of the new recombinases function in mammalian cells.

Results and Discussion

KD, R, B2, and B3 Yeast Recombinases Are Active in *Drosophila*. The ORFs predicted to encode the recombinases KD (from *Kluyveromyces drosophilarum*; ref. 35), R (from *Z. rouxii*; ref. 31), B2 (from *Zygosaccharomyces bailii*; ref. 37) and B3 (from *Zygosaccharomyces bisporus*; ref. 40) were synthesized with *Drosophila* codon usage. We wanted to decrease the half-lives of the recombinases to achieve tighter temporal control of activity and reduce potential toxicity. Therefore, a PEST sequence corresponding to residues 422–461 of the mouse ornithine decarboxylase gene (41) was appended at their C termini. The synthesized genes were cloned downstream of upstream activation sites (UAS) that bind the GAL4 transcription factor, thereby placing recombinase expression under the control of GAL4 (*Methods*; ref. 42).

Recombinase activity was assayed by using the excision reaction (Fig. 1*A*). We constructed a set of "stop cassettes" consisting of tandem *hsp70* and SV40 transcriptional terminators flanked by target sites specific for one of the recombinases. To create recombinase-specific reporter constructs, the stop cassettes were placed between 20 UAS sites and the coding sequence for a membrane-targeted, codon-optimized myristoylated

Author contributions: A.N., B.D.P., K.S., and G.M.R. designed research; A.N., B.D.P., and K.S. performed research; G.M.R. wrote the paper; A.N. tested the activity of the constructs in flies; B.D.P. proposed the use of these recombinases and made constructs; and K.S. tested the activity of the constructs in mice.

The authors declare no conflict of interest.

Freely available online through the PNAS open access option.

[1]A.N. and B.D.P. contributed equally to this work.

[2]To whom correspondence should be addressed. E-mail: rubing@janelia.hhmi.org.

This article contains supporting information online at www.pnas.org/lookup/suppl/doi:10.1073/pnas.1111704108/-/DCSupplemental.

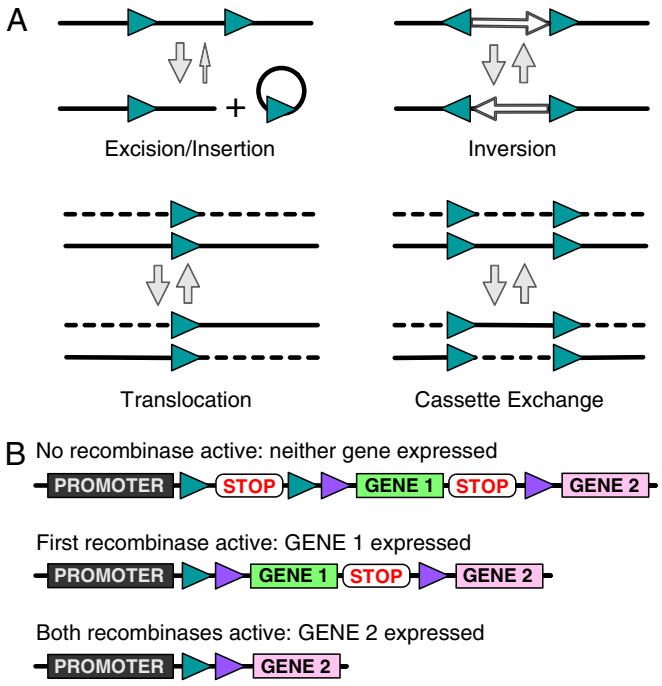

Fig. 1. Modifying genome structure and gene expression with site-specific recombinases. (*A*) Four types of reaction are diagramed. The target sites recognized by the recombinases are indicated by the colored triangles, and the black lines represent genomic DNA. In the excision/insertion reaction, a segment of DNA between two tandemly arranged target sites can be excised as a circular molecule. The reverse reaction, insertion, occurs with much lower efficiency. In the inversion reaction, a segment of DNA between two oppositely oriented target sites can undergo one or more cycles of inversion. In the translocation reaction, a segment of a chromosome arm distal to the centromere is exchanged between homologs in a diploid organism. In the cassette exchange reaction, a linear segment of DNA is exchanged between two DNA molecules. (*B*) An example of the use of two recombinases with distinct target sites (represented by the different colored triangles) to perform a genetic intersection (2).

Red Fluorescent Protein (pJFRC72; refs. 43 and 44). RFP expression from these constructs would be expected only if the KD, R, B2, or B3 recombinases were able to "kick-out," "rip-out," "bail-out," or "blow-out" their respective stop cassettes by excisional recombination.

Coexpression of each recombinase, under the control of 20XUAS sites (pJFRC7; ref. 43), and its cognate stop-cassette reporter using the pan-neuronal elav-GAL4 driver resulted in broad RFP expression in neurons; no RFP was observed in the absence of the construct encoding the recombinase. These results demonstrated that all four recombinases were active in *Drosophila*. We next asked if recombination went to completion, that is, whether the stop cassette excised in all recombinase-expressing cells. For this purpose, we used a more specific GAL4 driver line, R31F10 (constructed as described in ref. 45), which expresses in a single cell, the T1 neuron, in each of the 800 columns that comprise the medulla of the adult optic lobe. In a tangential section through the M2 layer of the medulla, a grid of T1 terminals is observed. The processes of different T1 neurons in this array do not overlap with each other, allowing us to score individual cells and determine the percentage in which an excision event had occurred (Fig. 2). High levels of recombinase expression resulted in the excision reaction going to completion for each of the four recombinases (Table 1). We also found that 3XUAS recombinase constructs, which we estimate express less than one-fifth the recombinase of the 20XUAS constructs used above (43), still result in complete, or nearly complete, excision for the three recombinases tested (B2, B3, KD).

Three additional yeast recombinases have been described; we did not try TD1 (46), and our initial attempts to use SM (34) and KW (34) were unsuccessful. In addition to the yeast recombinases, we also tested the ability of Dre, a recombinase closely related to Cre, to work in *Drosophila*. Dre showed only moderate efficiency in *Drosophila*; we were only able to get the excision reaction to go to ≈70% (179/269) completion. However, we found that Dre did not demonstrate the toxicity associated with Cre (see below). Thus, Dre would be a useful recombinase for applications where low efficiency is desired, such as stochastic cell labeling. We did not evaluate other members of the Cre family of recombinases, such as those recently described in *Vibrio* and *Shewanella* species (47).

During the course of this work, we used two different versions of FLP that differ in the amino acid residue at position 5, having either a glycine (G; ref. 6) or an aspartic acid (D; ref. 48). Although these two versions have not been distinguished in published reports describing the use of FLP in *Drosophila*, we found that the version containing an aspartic acid was >10 times more active based on the ability of hsFLP constructs encoding each version to induce excision of an FRT-flanked stop cassette under parallel conditions in the T1 medulla neuron. We observed an average of 6.5 excisions per optic lobe with the G5 FLP and 289 with the D5 FLP.

Together with FLP, the Recombinases We Analyzed Comprise Four Non–Cross-Reacting Recombinase-Target Site Pairs. We next assayed the ability of the recombinases to recognize each other's target sites and those of the FLP recombinase. We constructed *Drosophila* lines that paired all combinations of the FLP, KD, R, B2, and B3 recombinases and target sites. B2 and R showed partial cross-reaction, but all other noncognate pairs of recombinases and target sites were inactive (Fig. 2 and Table 1), even when the recombinases were expressed at several times the level needed to go to completion on their cognate sites.

Unlike Cre, FLP and the Other Yeast Recombinases Do Not Show Toxicity. Flies that expressed Cre-recombinase at high levels (20XUAS, pJFRC7; ref. 43) under the control of the pan-neural driver elav-GAL4 either did not reach the adult stage or were extremely uncoordinated and short-lived. By contrast, no obvious morphological or motility phenotypes were observed in otherwise identical crosses with 20XUAS KD, R, B2, B3, FLP, or Dre, or lower levels of Cre (3XUAS, pJFRC4; ref. 43). Similarly when flies homozygous for a 20XUAS recombinase were crossed to flies heterozygous for the ubiquitous driver tubulin-GAL4 (11) and a balancer chromosome (TM6B), we recovered tubulin-GAL4/20XUAS recombinase and balancer/20XUAS recombinase flies in roughly the expected 1:1 ratio for Dre (68:68), Flp (55:73), R (66:46), B2 (96:87), B3 (54:38), and KD (65:35). However, for Cre, no tubulin-GAL4/20XUAS recombinase progeny were recovered (0:79). Consistent with these results, high-level expression of Cre—but not the other recombinases—in the developing and adult eye using pGMR-GAL4 (49) resulted in strong defects in both external eye morphology and the arrangement of cells seen in sections cut through the retina. The lack of detectable toxicity resulting from expression of the yeast recombinases is more striking when we consider that the 20XUAS recombinase constructs used in these experiments are estimated to produce approximately fivefold more recombinase than needed to drive an excision reaction to apparent completion.

B3 and KD Recombinases Show Activity in Mammalian Cells. We prescreened the KD, R, B2, and B3 recombinases for activity in cultured Chinese hamster ovary (CHO) cells at 37 °C by cotransfecting CMV-GAL4::p65 with a UAS recombinase con-

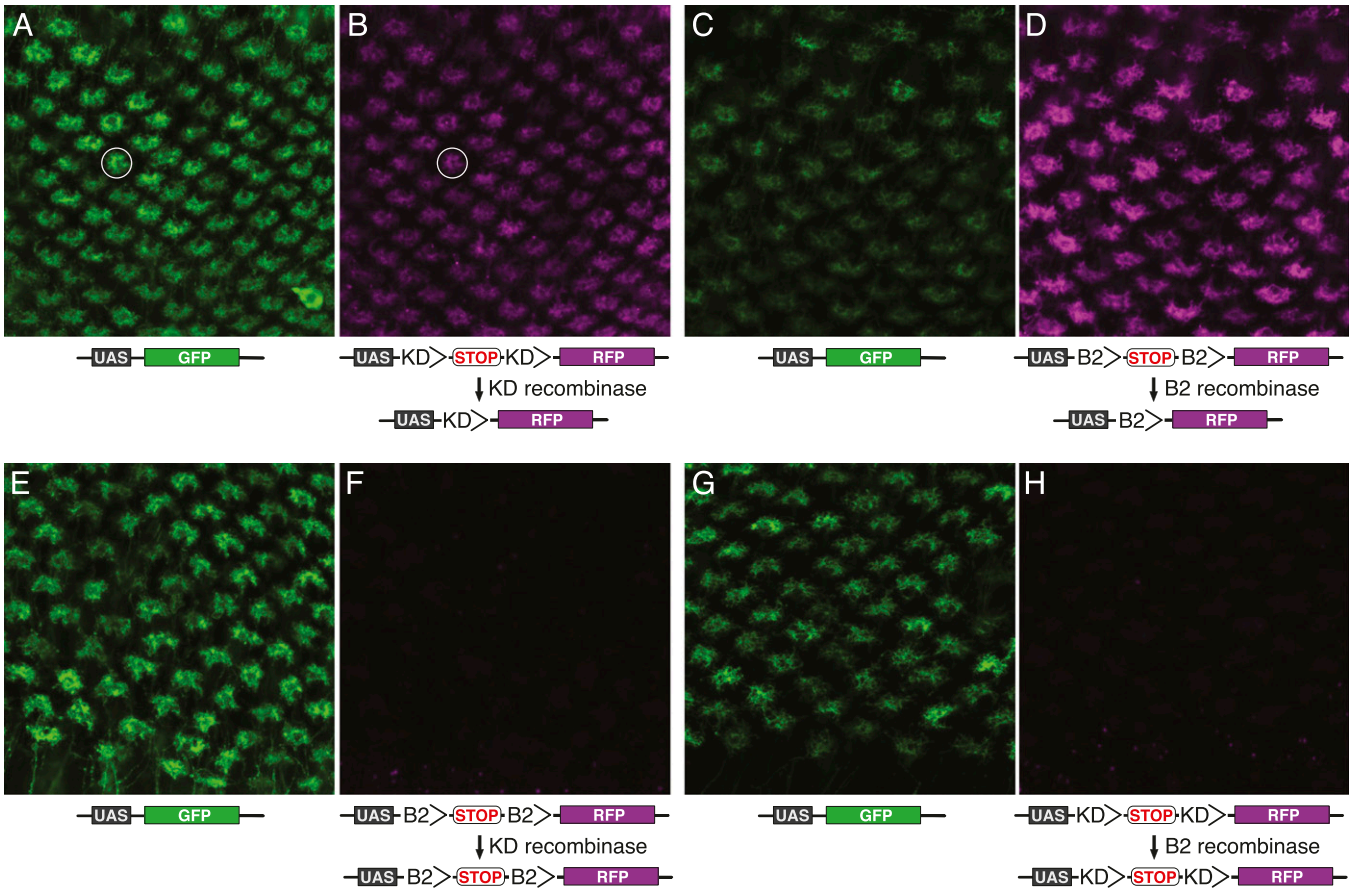

Fig. 2. Measuring recombinase activity and cross-reactivity. The images show projections of series of optical cross-sections through layer M2 of the medulla, a part of the optic lobes of *Drosophila* that is organized in regular vertical columns. The tangential orientation of the sections was chosen to reveal an array of columns. Examples from animals of differing genotypes are shown; each section is shown twice, GFP in green in *A*, *C*, *E*, and *G* or RFP in magenta in *B*, *D*, *F*, and *H*. Expression is driven in a single T1 cell in each column by the GAL4 driver line R31F10 and can be visualized by expression of GFP from a 10XUAS-mCD8::GFP construct (pJFRC2; ref. 43). To assay for the activity of a recombinase, a second reporter construct is included from which expression of RFP is observed only when a transcriptional stop cassette flanked by the target sites for a specific recombinase is excised. In *A* and *B*, the activity of the KD recombinase on its cognate target sites ("KD>" in the diagram shown in *B*, below the micrograph) is demonstrated. Note that RFP expression is observed in each of the ≈50 cells present in this field of view, indicating that the excision of the stop cassette by the recombinase has gone to completion; the neuronal processes of the same single cell are delineated in *A* and *B* by the white circle; the cell bodies of this and the other T1 cells are located outside the optical sections shown. In *C* and *D*, the ability of the B2 recombinase to recognize its cognate target sites (B2>) is shown; again the excision reaction appears to have gone to completion because the same cells can be seen in *C*, where expression of GFP does not require recombinase action, and in *D*, where expression of RFP is seen only in cells where recombinase action has led to removal of the stop cassette. The experiments presented in *E*–*H* show that the two recombinases show no detectable activity on each other's target sites. The KD recombinase is unable to remove a stop cassette flanked by B2 recombinase target sites (*E* and *F*), and the B2 recombinase is unable to remove a stop cassette flanked by KD recombinase target sites (*G* and *H*).

struct and its cognate stop-cassette reporter construct. These preliminary experiments suggested that B3 and KD were considerably more active under these conditions than R and B2. To further confirm B3 and KD activity, CHO cells were transfected with four plasmids: CMV-GAL4::p65 to drive transcription of the genes encoded by the other plasmids; 10XUAS-myr::GFP (pJFRC12; ref. 43) to provide a measure of transfection efficiency; 20XUAS B3 or 20XUAS KD recombinase; and a reporter construct with the appropriate stop cassette between the UAS sites and the RFP gene (Fig. 3). Recombinase activity was estimated as the fraction of GFP-expressing cells that also express RFP after correction for the recombination-independent background expression of RFP observed in some cells (Fig. 3*B*). Although the need to subtract this background (< 10% of transfected cells for both KD and B3) limited the precision with which we could estimate recombinase efficiency, these data demonstrate that both B3 (65% of transfected cells showing excision of the stop cassette) and KD (32%) were functional in mammalian cells at 37 °C, with B3 appearing more active than KD.

Based on these initial results, we tested the B3 and KD recombinases in cortical neurons in the mouse brain. Layer 2/3 progenitor cells were transduced by in utero electroporation

Table 1. Specificity of target site recognition by recombinases measured as percent of cells showing an excision event

	Recombinase				
Target	B2	B3	KD	R	FLP
B2RT	99.9	<0.1	<0.1	36	<0.1
B3RT	<0.1	99.9	<0.1	<0.1	<0.1
KDRT	<0.1	<0.1	99	<0.1	<0.1
RSRT	0.9	<0.1	<0.1	96	<0.1
FRT	<0.1	<0.1	<0.1	<0.1	91

Excision events were measured by using the assay shown in Fig. 2 (*Methods*). The values presented are based on scoring >1,000 cells for each combination of recombinase and target site. The stronger D5 version of FLP was used in these experiments.

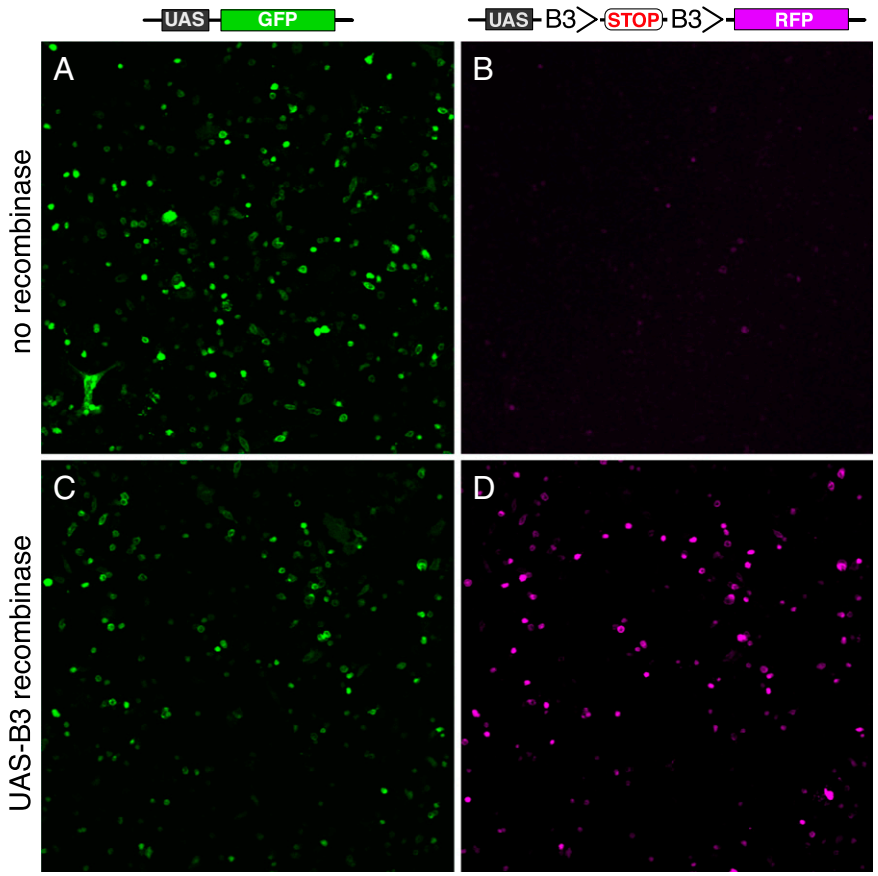

Fig. 3. Activity of the B3 recombinase in cultured Chinese hamster ovary cells. Images of cultured Chinese hamster ovary cells are shown. *A* and *C* have been imaged to reveal GFP fluorescence, and *B* and *D* show RFP fluorescence. Cells in all images have been transfected with a plasmid that expresses the transcriptional activator GAL4, a plasmid that expresses membrane localized GFP in response to GAL4 (which serves to identify those cells that have been successfully transfected) and a UAS–B3RT–stop cassette–B3RT–RFP construct. RFP expression is only expected if B3 recombinase is expressed and is able to remove the stop cassette, which is flanked by B3 recombination targets, allowing transcription of the RFP gene. A construct encoding the B3 recombinase (UAS-B3 recombinase) was included in the mixture of transfected DNAs in *C* and *D*. The observation that a high proportion of the cells marked by GFP in *C* show RFP fluorescence in *D* indicates that the B3 recombinase is active in CHO cells. A background of cells that express RFP weakly is seen in *B*; presumably, this expression results from either transcription reading through the stop cassette or internal transcriptional initiation.

(refs. 50 and 51; embryonic day 16) with two separate plasmids. One plasmid drove expression of B3 or KD under control of the synapsin promoter (refs. 52 and 53; syn-B3 and syn-KD, respectively). The other plasmid contained the tdTomato gene (44) driven by the CAG promoter (54–56), but separated from the promoter by either the B3 or KD-specific stop cassette (CAG_BlownOUT_tdTomato and CAG_KickedOUT_tdTomato, respectively).

Brains were harvested from mature mice (28–35 d postnatal) and inspected for tdTomato expression. Mouse brains that expressed matching recombinases and reporter constructs typically harbored numerous red fluorescent neurons in layer 2/3 (syn-B3 plus CAG_BlownOUT_tdTomato, 9/10 mice; syn-KD plus CAG_KickedOUT_tdTomato, 5/7 mice). Neurons were strongly labeled with tdTomato without obvious signs of toxicity. The fluorescent neurons appeared to have normal dendritic morphology, and local and long-range axonal projections (Fig. 4). The absence of fluorescence in some brains is likely explained by the failure rate, ≈20%, of the in utero electroporation technique. These experiments show that KD and B3 are active in the mouse brain. Fluorescent neurons were never detected in brains transduced with unmatched recombinases and reporter constructs (syn-B3 plus CAG_KickedOUT_tdTomato, 0/5 mice; syn-KD plus CAG_BlownOUT_tdTomato, 0/3 mice), suggesting that, as in flies, B3 and KD are not cross-reactive.

Further experiments will be required to compare the activity and toxicity of these recombinases with that of FLP and Cre. In the case of FLP, engineering the protein to be more thermostable significantly increased activity (57, 58) and similar efforts could be applied here if necessary. However, based on the cell culture assays, it appears that B3 is already highly active at 37 °C.

Concluding Remarks

A variety of methods that are based on site-specific recombination have been used in *Drosophila* (3, 7–11), but the ability to apply multiple methods, or methods that require multiple recombinases, in the same animal has been severely limited by the lack of a set of non–cross-reacting, nontoxic recombinases. The results we present here remove this limitation and establish a robust toolkit of four distinct recombinases—KD, B2, B3, and FLP—for use in *Drosophila*. Each has sufficient activity to drive an excision reaction to completion without displaying detectable cross-reactivity or obvious toxicity. We also show that at least two of the recombinases, KD and B3, are active in mammalian tissues.

Methods

Molecular Biology and *Drosophila* Genetics. Constructs for use in *Drosophila* and transgenic fly lines were generated by standard methods as described in refs. 43 and 45; see *SI Methods* for details. *Drosophila* codon-optimized

GENETICS

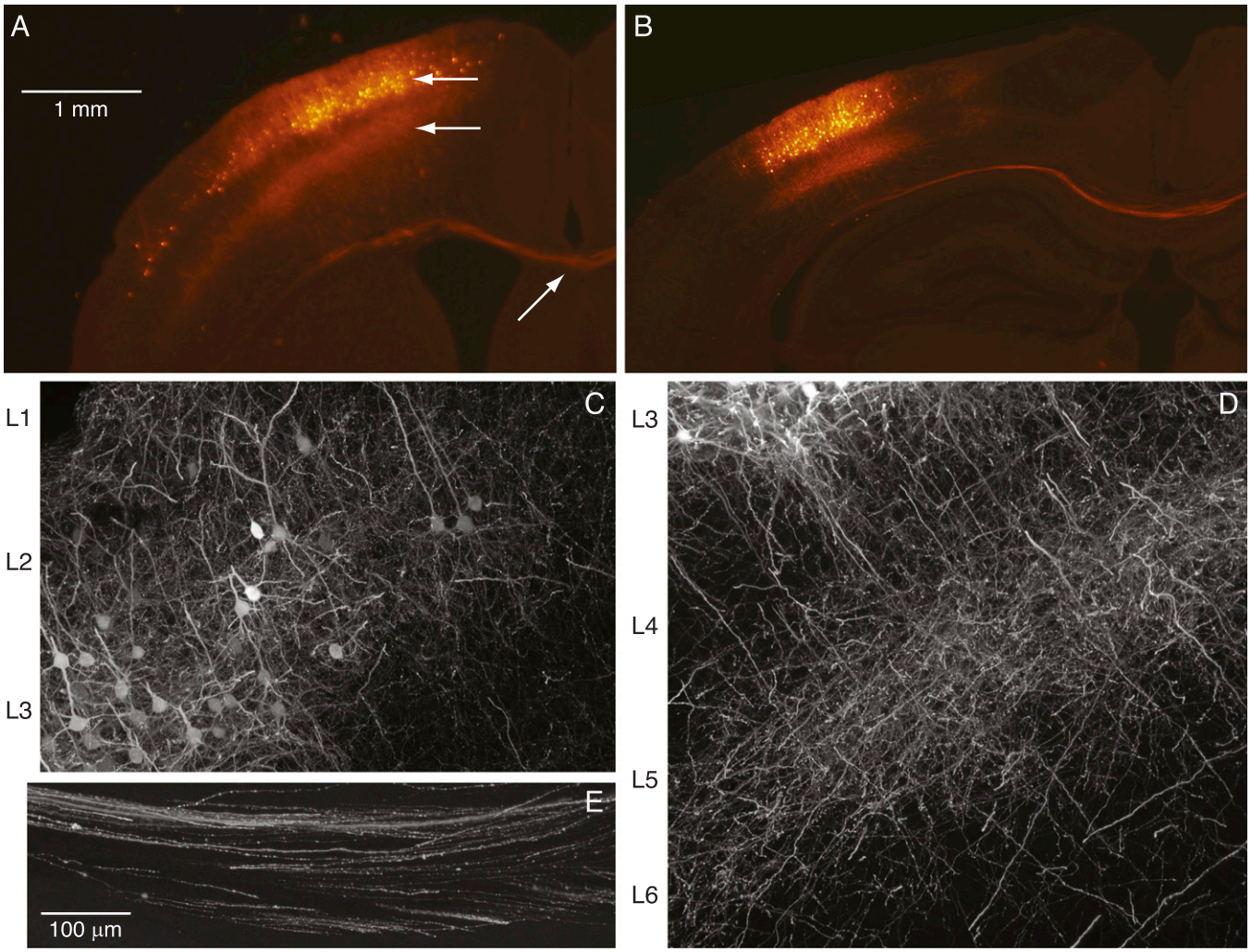

Fig. 4. Activity of the B3 and KD recombinases in mice. Plasmids encoding the recombinase and a reporter of recombinase activity were introduced into embryonic day 16 embryos by in utero electroporation. Removal of the transcriptional stop cassette flanked by recombinase target sites causes tdTomato expression. Imaging of tdTomato fluorescence was in brain section (thickness, 50 microns) from an adult mouse. (*A*) KD recombinase and a reporter for KD activity were introduced into layer 2/3 cells. Imaging was with a macroscope. Arrows (from top to bottom) correspond to layer 2/3 pyramidal cells, their local axons in layer 5, and their long-range axons in the *corpus callosum*. (Scale bar: 1 mm.) (*B*) Same as *A* for the B3 recombinase. (*C*–*E*) Different regions of interest in one brain section imaged with confocal microscopy (B3 recombinase): (*C*) dendritic arbors of layer 2/3 pyramidal neurons; (*D*) local axonal projections from layer 2/3 neurons in layer 5; (*E*) long-range projections in the *corpus callosum*. (Scale bar: 100 microns.)

recombinases and their cognate recognition sites were synthesized by DNA2.0, Inc.; complete DNA sequences are given in Fig. S1, Fig. S2, and Fig. S3. Plasmid constructs are available from Addgene.

Imaging of Optic Lobes. Optic lobes from 5- to 10-d adult flies, mounted in an appropriate orientation, were imaged on a Zeiss LSM 710 confocal microscope by using a 20× 0.8 NA objective. For further details, see *SI Methods*.

CHO assays. CHO-K1 cells (ATCC CCL-61) were plated at a density of 4×10^5 in 35 mm MatTEk culture plates (Mattek). The next day, a total of 4 μg of plasmid DNA in 250 μL of Opti-MEM I Reduced Serum Medium (Invitrogen) were combined with Lipofectamine 2000 (Invitrogen) and used to transfect CHO-K1 cells according to manufacturer recommendations. GFP and RFP fluorescence were visualized ≈24 h after transfection by using a Zeiss LSM 510 confocal microscope.

In Vivo Mouse Assays. Approximately 1 μL of DNA solution consisting of a mixture of plasmids in a 1:1 ratio at a final DNA concentration of 2 μg/μL was injected into the right lateral ventricle of each embryo (embryonic day 16 C57BL/6J mice) and then electroporated as described in *SI Methods*. The plasmids used for mouse in utero electroporation were based on an Adeno-associated virus (AAV) backbone (56); see *SI Methods* for details.

ACKNOWLEDGMENTS. We thank Tanya Wolff for sectioning and morphological analysis of adult *Drosophila* eyes; Todd Laverty and the Janelia Farm Drosophila shared resource for stock maintenance; Helen White and Sarah Winfrey for assistance with the CHO cell transfection experiments; Torrey Gallagher for construction of AAV vectors; Amy Hu for preparing mouse brain sections, Kevin McGowan and the Janelia Farm Molecular Biology shared resource for DNA sequencing; Genetic Services Inc. for generation of the transgenic flies; and Tzumin Lee, Jim Truman, David Anderson, Charles Zuker, and Larry Zipursky for comments on the manuscript. This work was supported by the Howard Hughes Medical Institute.

1. García-Otín AL, Guillou F (2006) Mammalian genome targeting using site-specific recombinases. *Front Biosci* 11:1108–1136.
2. Dymecki SM, Kim JC (2007) Molecular neuroanatomy's "Three Gs": A primer. *Neuron* 54:17–34.
3. Luan H, White BH (2007) Combinatorial methods for refined neuronal gene targeting. *Curr Opin Neurobiol* 17:572–580.
4. Birling MC, Gofflot F, Warot X (2009) Site-specific recombinases for manipulation of the mouse genome. *Methods Mol Biol* 561:245–263.
5. Grindley ND, Whiteson KL, Rice PA (2006) Mechanisms of site-specific recombination. *Annu Rev Biochem* 75:567–605.
6. Hartley JL, Donelson JE (1980) Nucleotide sequence of the yeast plasmid. *Nature* 286: 860–865.

7. Golic KG, Lindquist S (1989) The FLP recombinase of yeast catalyzes site-specific recombination in the Drosophila genome. *Cell* 59:499–509.
8. Struhl G, Basler K (1993) Organizing activity of wingless protein in Drosophila. *Cell* 72: 527–540.
9. Golic KG (1991) Site-specific recombination between homologous chromosomes in Drosophila. *Science* 252:958–961.
10. Xu T, Rubin GM (1993) Analysis of genetic mosaics in developing and adult Drosophila tissues. *Development* 117:1223–1237.
11. Lee T, Luo L (1999) Mosaic analysis with a repressible cell marker for studies of gene function in neuronal morphogenesis. *Neuron* 22:451–461.
12. Awatramani R, Soriano P, Rodriguez C, Mai JJ, Dymecki SM (2003) Cryptic boundaries in roof plate and choroid plexus identified by intersectional gene activation. *Nat Genet* 35:70–75.
13. Farago AF, Awatramani RB, Dymecki SM (2006) Assembly of the brainstem cochlear nuclear complex is revealed by intersectional and subtractive genetic fate maps. *Neuron* 50:205–218.
14. Voziyanov Y, Konieczka JH, Stewart AF, Jayaram M (2003) Stepwise manipulation of DNA specificity in Flp recombinase: Progressively adapting Flp to individual and combinatorial mutations in its target site. *J Mol Biol* 326:65–76.
15. Hadjieconomou D, et al. (2011) Flybow: Genetic multicolor cell labeling for neural circuit analysis in Drosophila melanogaster. *Nat Methods* 8:260–266.
16. Nagy A (2000) Cre recombinase: The universal reagent for genome tailoring. *Genesis* 26:99–109.
17. Sauer B, Henderson N (1988) Site-specific DNA recombination in mammalian cells by the Cre recombinase of bacteriophage P1. *Proc Natl Acad Sci USA* 85:5166–5170.
18. Orban PC, Chui D, Marth JD (1992) Tissue- and site-specific DNA recombination in transgenic mice. *Proc Natl Acad Sci USA* 89:6861–6865.
19. Siegal ML, Hartl DL (1996) Transgene Coplacement and high efficiency site-specific recombination with the Cre/loxP system in Drosophila. *Genetics* 144:715–726.
20. Heidmann D, Lehner CF (2001) Reduction of Cre recombinase toxicity in proliferating Drosophila cells by estrogen-dependent activity regulation. *Dev Genes Evol* 211: 458–465.
21. Schmidt EE, Taylor DS, Prigge JR, Barnett S, Capecchi MR (2000) Illegitimate Cre-dependent chromosome rearrangements in transgenic mouse spermatids. *Proc Natl Acad Sci USA* 97:13702–13707.
22. Forni PE, et al. (2006) High levels of Cre expression in neuronal progenitors cause defects in brain development leading to microencephaly and hydrocephaly. *J Neurosci* 26:9593–9602.
23. Schmidt-Supprian M, Rajewsky K (2007) Vagaries of conditional gene targeting. *Nat Immunol* 8:665–668.
24. Coppoolse ER, et al. (2003) Cre recombinase expression can result in phenotypic aberrations in plants. *Plant Mol Biol* 51:263–279.
25. Sauer B, McDermott J (2004) DNA recombination with a heterospecific Cre homolog identified from comparison of the pac-c1 regions of P1-related phages. *Nucleic Acids Res* 32:6086–6095.
26. Anastassiadis K, et al. (2009) Dre recombinase, like Cre, is a highly efficient site-specific recombinase in E. coli, mammalian cells and mice. *Dis Model Mech* 2:508–515.
27. Groth AC, Olivares EC, Thyagarajan B, Calos MP (2000) A phage integrase directs efficient site-specific integration in human cells. *Proc Natl Acad Sci USA* 97:5995–6000.
28. Groth AC, Fish M, Nusse R, Calos MP (2004) Construction of transgenic Drosophila by using the site-specific integrase from phage phiC31. *Genetics* 166:1775–1782.
29. Bateman JR, Lee AM, Wu CT (2006) Site-specific transformation of Drosophila via phiC31 integrase-mediated cassette exchange. *Genetics* 173:769–777.
30. Turan S, et al. (2011) Recombinase-mediated cassette exchange (RMCE): Traditional concepts and current challenges. *J Mol Biol* 407:193–221.
31. Araki H, et al. (1985) Molecular and functional organization of yeast plasmid pSR1. *J Mol Biol* 182:191–203.
32. Yang SH, Jayaram M (1994) Generality of the shared active site among yeast family site-specific recombinases. The R site-specific recombinase follows the Flp paradigm [corrected]. *J Biol Chem* 269:12789–12796.
33. Onouchi H, et al. (1991) Operation of an efficient site-specific recombination system of Zygosaccharomyces rouxii in tobacco cells. *Nucleic Acids Res* 19:6373–6378.
34. Volkert FC, Wilson DW, Broach JR (1989) Deoxyribonucleic acid plasmids in yeasts. *Microbiol Rev* 53:299–317.
35. Chen XJ, Saliola M, Falcone C, Bianchi MM, Fukuhara H (1986) Sequence organization of the circular plasmid pKD1 from the yeast Kluyveromyces drosophilarum. *Nucleic Acids Res* 14:4471–4481.
36. Toh-e A, Araki H, Utatsu I, Oshima Y (1984) Plasmids resembling 2-micrometers DNA in the osmotolerant yeasts Saccharomyces bailii and Saccharomyces bisporus. *J Gen Microbiol* 130:2527–2534.
37. Utatsu I, Sakamoto S, Imura T, Toh-e A (1987) Yeast plasmids resembling 2 micron DNA: Regional similarities and diversities at the molecular level. *J Bacteriol* 169: 5537–5545.
38. Utatsu I, Utsunomiya A, Toh-e A (1986) Functions encoded by the yeast plasmid pSB3 isolated from Zygosaccharomyces rouxii IFO 1730 (formerly Saccharomyces bisporus var. mellis). *J Gen Microbiol* 132:1359–1365.
39. Araki H, et al. (1992) Site-specific recombinase, R, encoded by yeast plasmid pSR1. *J Mol Biol* 225:25–37.
40. Toh-e A, Utatsu I (1985) Physical and functional structure of a yeast plasmid, pSB3, isolated from Zygosaccharomyces bisporus. *Nucleic Acids Res* 13:4267–4283.
41. Loetscher P, Pratt G, Rechsteiner M (1991) The C terminus of mouse ornithine decarboxylase confers rapid degradation on dihydrofolate reductase. Support for the pest hypothesis. *J Biol Chem* 266:11213–11220.
42. Brand AH, Perrimon N (1993) Targeted gene expression as a means of altering cell fates and generating dominant phenotypes. *Development* 118:401–415.
43. Pfeiffer BD, et al. (2010) Refinement of tools for targeted gene expression in Drosophila. *Genetics* 186:735–755.
44. Shaner NC, et al. (2004) Improved monomeric red, orange and yellow fluorescent proteins derived from Discosoma sp. red fluorescent protein. *Nat Biotechnol* 22: 1567–1572.
45. Pfeiffer BD, et al. (2008) Tools for neuroanatomy and neurogenetics in Drosophila. *Proc Natl Acad Sci USA* 105:9715–9720.
46. Blaisonneau J, Sor F, Cheret G, Yarrow D, Fukuhara H (1997) A circular plasmid from the yeast Torulaspora delbrueckii. *Plasmid* 38:202–209.
47. Suzuki E, Nakayama M (2011) VCre/VloxP and SCre/SloxP: New site-specific recombination systems for genome engineering. *Nucleic Acids Res* 39:e49.
48. Babineau D, et al. (1985) The FLP protein of the 2-micron plasmid of yeast. Purification of the protein from Escherichia coli cells expressing the cloned FLP gene. *J Biol Chem* 260:12313–12319.
49. Freeman M (1996) Reiterative use of the EGF receptor triggers differentiation of all cell types in the *Drosophila* eye. *Cell* 87:651–660.
50. Saito T, Nakatsuji N (2001) Efficient gene transfer into the embryonic mouse brain using in vivo electroporation. *Dev Biol* 240:237–246.
51. Petreanu L, Huber D, Sobczyk A, Svoboda K (2007) Channelrhodopsin-2-assisted circuit mapping of long-range callosal projections. *Nat Neurosci* 10:663–668.
52. Kügler S, et al. (2001) Neuron-specific expression of therapeutic proteins: Evaluation of different cellular promoters in recombinant adenoviral vectors. *Mol Cell Neurosci* 17:78–96.
53. Südhof TC (1990) The structure of the human synapsin I gene and protein. *J Biol Chem* 265:7849–7852.
54. Niwa H, Yamamura K, Miyazaki J (1991) Efficient selection for high-expression transfectants with a novel eukaryotic vector. *Gene* 108:193–199.
55. Gray NW, Weimer RM, Bureau I, Svoboda K (2006) Rapid redistribution of synaptic PSD-95 in the neocortex in vivo. *PLoS Biol* 4:e370.
56. Petreanu L, Mao T, Sternson SM, Svoboda K (2009) The subcellular organization of neocortical excitatory connections. *Nature* 457:1142–1145.
57. Buchholz F, Angrand PO, Stewart AF (1998) Improved properties of FLP recombinase evolved by cycling mutagenesis. *Nat Biotechnol* 16:657–662.
58. Rodríguez CI, et al. (2000) High-efficiency deleter mice show that FLPe is an alternative to Cre-loxP. *Nat Genet* 25:139–140.

Supporting Information

Nern et al. 10.1073/pnas.1111704108

SI Methods

Molecular Biology. *Drosophila* codon-optimized recombinases and their cognate recognition sites were synthesized by DNA2.0, Inc. The coding sequences for the recombinases are shown in Fig. S1 for B3, KD, and B2 and Fig. S2 for R and FLP. The sequences of the stop cassettes used in this work for the B3, KD, B2, RS, and FLP stop cassettes are shown in Fig. S3.

To construct pBPhsFlp1 and pBPhsFlp2 sequences encoding yeast FLP were amplified from the pUAS-Flp vector (ref. 1; obtained from the Drosophila Genome Resource Center) to contain an optimal translation sequence and cloned as a 5′ KpnI–3′ Avr2 fragment into a modified pBDP (2) vector that contains the *Hsp70Bb* Heat Shock Promoter (−194 to +237) and 337-bp terminator (ref. 3; CG31359). Two variants of the FLP coding sequence were recovered; pBPhsFlp1 contains a D5 residue and pBPhsFlp2 a G5 residue. Sequences have been reported for the yeast Flp gene that encode either G5 or D5 (4, 5).

All recombinases used in the UAS vectors were synthesized to include a C-terminal PEST sequence; nuclear localization sequences were not added. The same recombinase genes (*Drosophila*-codon optimized and including the PEST sequence) and stop cassettes were used in flies, CHO cells, and mice. RFP was used as a reporter in the stop cassettes for B2, B3, KD, and R; GFP in the cassettes for Cre, Dre, and FLP.

The plasmids used for mouse in utero electroporation were based on an AAV virus backbone (6). The modular cassettes BlownOUT and KickedOUT were cloned into the BamHI site of the AAV-CAG_tdTomato vector (gift of Jinny Kim, Janelia Farm Research Campus) to generate CAG_BlownOUT_tdTomato and CAG_KickedOUT_tdTomato. AAV-syn-B3:PEST and AAV-syn-KD:PEST were constructed by substituting the *Drosophila*-codon optimized B3 and KD genes, respectively, for the GCaMP3 gene in the AAV-syn-GCaMP3 construct (7).

***Drosophila* Transgenics and Genetics.** Transgenic fly lines were generated as described (2, 8). For assaying recombinase activity, flies with appropriate stop-cassette reporter constructs inserted in attP40 and R31F10-GAL4 (in attP2) or elav-GAL4 (C155; ref. 9) were crossed to UAS recombinase flies (in attP2). To visualize the entire R31F10 pattern, a 10XUAS-mCD8::GFP reporter (pJFRC2 in attP40) was included in some cases. For testing 3XUAS recombinase constructs (in attP40), stop-cassette reporters in VK00005 and attP2 were used. For comparing the D5 and G5 FLP variants, low levels of FLP were expressed under hs-promoter control (using pBPhsFlp1 or pBPhsFlp2 in attP2) by raising flies at 25 °C without additional heat shock. To test for toxicity of recombinase expression, UAS recombinase drivers in attP2 (20XUAS) were crossed to elav-GAL4 (C155; ref. 9), tubP-GAL4 (10), or GMR-GAL4 (11).

Imaging of Optic Lobes. Optic lobes from 5- to 10-d adult flies, mounted in an appropriate orientation, were imaged on a Zeiss LSM 710 confocal microscope by using a 20× 0.8 NA objective. To aid quantification of medulla columns with stop-cassette excision, two methods were used to visualize all medulla columns: To assay KD, B2, B3, and R activity and potential cross-reactivity of these recombinases, the entire medulla pattern of R31F10 was revealed by using mCD8 GFP (pJFRC2-10XUAS-IVS-mCD8::GFP). In this case, samples were mounted in PBS and native GFP and RFP fluorescence were imaged directly after dissection. For all other experiments, mAb24B10 (12) staining of R7 and R8 photoreceptor neurons was used as an indirect marker for the positions of T1 neurons, which, like R7 and R8, are present once per medulla column. For these experiments, brains were dissected in PBS, fixed with 2% formaldehyde in PBS for 1 h, washed several times with PBT (PBS + 0.5% TX-100), blocked with PBT with 5% goat serum and incubated with rabbit anti-GFP (Invitrogen; 1:1,000 dilution) or rabbit anti-ds-Red (Clontech; 1:1,000 dilution) plus mAb24B10 (ref. 12; Developmental Studies Hybridoma Bank; 1:20 dilution) overnight at 4 °C. Secondary antibodies were donkey anti-mouse DyLight 649 (1:500; Jackson Immunoresearch) and donkey anti-rabbit DyLight 488 (1:500; Jackson Immunoresearch). Samples were mounted in Slowfade Gold (Invitrogen). Eye sections to assess recombinase toxicity were prepared as described (13).

In Vivo Mouse Assays. Embryonic day 16 timed-pregnant C57BL/6J mice (Charles River) were deeply anesthetized by using an isoflurane-oxygen mixture [2% (vol/vol) isoflurane in O_2]. The uterine horns were exposed and ≈1 μL of DNA solution was pressure-injected through a pulled glass capillary tube into the right lateral ventricle of each embryo. The DNA solution contained a mixture of plasmids in a 1:1 ratio at a final concentration of 2 μg/μL. The head of each embryo was placed between custom-made tweezer electrodes, with the positive plate contacting the right side of the head. Electroporation (14, 15) was achieved with five square pulses (duration 50 ms, frequency 1 Hz, 40 V). Electroporated mice were perfused with cold saline and 4% paraformaldehyde and fixed overnight. Analysis of tdTomato expression was performed in 50-μm-thick brain sections.

1. Duffy JB, Harrison DA, Perrimon N (1998) Identifying loci required for follicular patterning using directed mosaics. *Development* 125:2263–2271.
2. Pfeiffer BD, et al. (2008) Tools for neuroanatomy and neurogenetics in Drosophila. *Proc Natl Acad Sci USA* 105:9715–9720.
3. Ingolia TD, Craig EA, McCarthy BJ (1980) Sequence of three copies of the gene for the major Drosophila heat shock induced protein and their flanking regions. *Cell* 21: 669–679.
4. Hartley JL, Donelson JE (1980) Nucleotide sequence of the yeast plasmid. *Nature* 286: 860–865.
5. Babineau D, et al. (1985) The FLP protein of the 2-micron plasmid of yeast. Purification of the protein from Escherichia coli cells expressing the cloned FLP gene. *J Biol Chem* 260:12313–12319.
6. Petreanu L, Mao T, Sternson SM, Svoboda K (2009) The subcellular organization of neocortical excitatory connections. *Nature* 457:1142–1145.
7. Tian L, et al. (2009) Imaging neural activity in worms, flies and mice with improved GCaMP calcium indicators. *Nat Methods* 6:875–881.
8. Pfeiffer BD, et al. (2010) Refinement of tools for targeted gene expression in Drosophila. *Genetics* 186:735–755.
9. Lin DM, Fetter RD, Kopczynski C, Grenningloh G, Goodman CS (1994) Genetic analysis of Fasciclin II in Drosophila: Defasciculation, refasciculation, and altered fasciculation. *Neuron* 13:1055–1069.
10. Lee T, Luo L (1999) Mosaic analysis with a repressible cell marker for studies of gene function in neuronal morphogenesis. *Neuron* 22:451–461.
11. Freeman M (1996) Reiterative use of the EGF receptor triggers differentiation of all cell types in the Drosophila eye. *Cell* 87:651–660.
12. Zipursky SL, Venkatesh TR, Teplow DB, Benzer S (1984) Neuronal development in the Drosophila retina: Monoclonal antibodies as molecular probes. *Cell* 36:15–26.
13. Wolff T (2000) Histological Techniques for the Drosophila eye, Part II: Adult. *Drosophila protocols*, eds Sullivan W, Ashburner M, Hawley RS (Cold Spring Harbor Lab Press, Cold Spring Harbor, NY), pp 229–243.
14. Petreanu L, Huber D, Sobczyk A, Svoboda K (2007) Channelrhodopsin-2-assisted circuit mapping of long-range callosal projections. *Nat Neurosci* 10:663–668.
15. Kügler S, et al. (2001) Neuron-specific expression of therapeutic proteins: evaluation of different cellular promoters in recombinant adenoviral vectors. *Mol Cell Neurosci* 17:78–96.
16. Cavener DR, Ray SC (1991) Eukaryotic start and stop translation sites. *Nucleic Acids Res* 19:3185–3192.

17. Carswell S, Alwine JC (1989) Efficiency of utilization of the simian virus 40 late polyadenylation site: effects of upstream sequences. *Mol Cell Biol* 9:4248–4258.

18. Brand AH, Perrimon N (1993) Targeted gene expression as a means of altering cell fates and generating dominant phenotypes. *Development* 118:401–415.

B3 Recombinase

CTCGAGAATCAAAATGAGCTCGTATATGGATCTTGTTGATGATGAACCAGCGACTTTGTACCATAAGTTCGTGGAGTGCT
TGAAAGCGGGCGAGAACTTCTGCGGAGACAAGCTGAGTGGAATTATTACCATGGCGATCCTTAAGGCAATCAAGGCGCTG
ACCGAAGTTAAAAAGACAACCTTTAACAAATATAAGACAACAATCAAGCAGGGCCTCCAGTATGACGTGGGTTCGTCGAC
TATCTCGTTTGTGTATCACTTGAAGGACTGTGATGAGCTGTCCAGGGGCTTGAGCGATGCCTTCGAGCCCTACAAATTCA
AAATTAAGTCGAATAAAGAGGCAACCTCGTTTAAGACTCTCTTTCGTGGCCCCTCGTTTGGCAGCCAGAAGAACTGGCGG
AAGAAAGAGGTGGACCGCGAGGTGGATAACTTGTTTCATAGCACCGAGACAGACGAATCGATTTTCAAATTCATCTTGAA
CACGTTGGATAGTATTGAGACACAAACGAACACGGATCGCCAAAAGACGGTGCTGACTTTCATCCTGTTGATGACATTTT
TCAACTGCTGTAGGAACAATGACCTGATGAACGTTGATCCCTCCACATTTAAGATTGTGAAAAACAAATTCGTCGGATAC
CTGCTGCAGGCTGAGGTCAAACAGACTAAGACACGCAAGTCGAGGAACATTTTCTTCTTTCCCATCCGCGAGAATCGATT
CGATCTGTTCCTGGCCTTGCACGATTTCTTCCGCACATGCCAGCCTACCCCAAAGTCGCGTCTTTCGGATCAAGTATCGG
AGCAGAAGTGGCAGCTTTTCCGAGATTCCATGGTCATTGATTACAACCGTTTCTTTAGGAAGTTTCCAGCTTCGCCTATT
TTCGCAATAAAGCACGGCCCCAAGTCCCATCTGGGCCGGCATCTGATGAACAGCTTTCTGCACAAGAATGAACTGGATTC
CTGGGCCAACTCCCTGGGCAACTGGAGCTCCTCCCAGAATCAACGCGAGTCCGGTGCGCGACTGGGCTACACCCACGGTG
GTCGAGATTTGCCACAGCCACTGTTCGGATTCCTGGCTGGCTACTGCGTTCGAAATGAAGAGGGCCACATCGTGGGCTTG
GGTCTGGAGAAGGACATTAATGATCTGTTTGACGGTATTATGGACCCACTTAATGAGAAGGAGGATACAGAGATTTGTGA
AAGCTACGGCGAGTGGGCCAAAATTGTGAGCAAGGATGTTCTGATATTTCTGAAGCGATATCATTCGAAGAACGCATGCC
GGCGATATCAGAACTCCACATTGTACGCACGTACGTTCCTTAAGACAGAGTCCGTCACCTTGAGCGGCTCCAAGGGAAGC
GAAGAGCCGAGCAGTCCCGTCAGGATTCCAATACTTAGTATGGGAAAAGCCTCCCCAAGCGAGGGCCGAAAGTTGCGTGC
CAGCGAACATGCCAACGATGATAATGAGATTGAGAAGATAGATTCGGATTCGTCGCAAAGCGAAGAGATACCTATCGAAA
TGTCCGACTCCGAGGACGAAACAACGGCAAGTAACATTAGCGGAATTTACCTGGACATGTCGAAAGCCAACTCCAACGTG
GTCTATTCCCCTCCGAGTCAGACTGGCCGTGCCGCCGGTGCCGGCCGTAAACGTGGCGTGGGTGGTCGCCGCACCGTTGA
GTCGAAGCGGCGGCGCGTCCTGGCACCAATTAACCGGGGATCCCATGGCTTCCCTCCAGAGGTGGAGGAGCAAGATGATG
GCACTCTCCCCATGAGCTGCGCTCAAGAGAGTGGCATGGATCGTCACCCCGCTGCTTGCGCCTCGGCTCGCATCAACGTG
TAATCTAGA

KD Recombinase

CTCGAGAATCAAAATGAGTACTTTTGCAGAAGCAGCGCATCTTACACCGCATCAATGTGCGAACGAAATCAACGAGATTC
TGGAAAGTGATACATTCAACATTAATGCGAAAGAAATACGCAACAAGTTGGCTAGTCTCTTTTCCATTCTTACCATGCAA
TCGCTGTCCATCCGTAGGGAAATGAAGATTAACACGTATCGTAGCTACAAGTCCGCAATCGGAAAATCCCTGAGCTTTGA
CAAGGATGACAAGATTATCAAATTCACTGTACGGCTGAGGAAGACCGAGAGTCTGCAGAAAGACATTGAAAGCGCACTCC
CGTCCTACAAAGTCGTTGTTTCGCCATTCAAAAACCAGGAGGTGTCGCTTTTCGATCGATACGAGGAAACCCACAAGTAC
GATGCGTCCATGGTGGGCCTCCAATTTACGAACATTCTCAGCAAGGAGAAAGACATCTGGAAAATCGTTAGCCGAATCGC
TTGCTTCTTCGATCAGTCGTGCGTGACGACCACGAAGCGAGCGGAGTACCGCCTGCTTCTGCTGGGAGCCGTAGGTAACT
GTTGCCGTTATAGCGATCTCAAAAATCTGGACCCCCGGACCTTTGAGATTTACAACAATTCCTTCTTGGGACCAATCGTG
CGGGCCACGGTTACAGAGACAAAGAGTCGCACAGAGCGATATGTGAACTTTTACCCAGTGAATGGTGATTGCGATCTGTT
GATTTCCCTCTACGATTACCTCCGAGTTTGCTCCCCGATCGAGAAGACTGTGTCGAGCAATCGGCCGACAAACCAGACGC
ACCAGTTCCTCCCGGAATCCCTTGCGCGGACCTTCAGCCGCTTCCTGACCCAGCACGTTGACGAGCCAGTCTTCAAGATT
TGGAACGGCCCGAAGTCGCACTTCGGTCGGCACCTGATGGCTACCTTCTTGTCGCGCTCCGAAAAGGGAAAGTATGTTTC
CTCCCTGGGCAACTGGGCAGGTGACCGCGAAATCCAGAGCGCCGTCGCGCGCTCCCACTACTCGCATGGTTCCGTTACCG
TTGACGACCGGGTCTTTGCATTCATATCGGGATTTTACAAAGAAGCCCCGCTGGGTTCCGAGATTTATGTGTTGAAGGAC
CCCTCCAACAAGCCACTCAGCAGGGAGGAGCTGCTTGAGGAGGAGGGCAACTCGCTCGGAAGTCCCCCACTGAGTCCTCC
CTCCTCGCCCCGACTGGTGGCCCAGTCGTTCAGTGCACACCCGTCGCTGCAACTCTTCGAACAGTGGCACGGCATCATCA
GCGACGAGGTCCTGCAATTTATTGCGGAATATAGGCGCAAGCACGAGCTGCGGAGCCAGCGTACGGTGGTTGCAGGATCC
CATGGCTTCCCTCCAGAGGTGGAGGAGCAAGATGATGGCACTCTCCCCATGAGCTGCGCTCAAGAGAGTGGCATGGATCG
TCACCCCGCTGCTTGCGCCTCGGCTCGCATCAACGTGTAATCTAGA

B2 Recombinase

CTCGAGAATCAAAATGTCGGAATTTAGTGAGTTGGTACGTATCTTGCCTTTGGATCAGGTTGCGGAGATCAAACGTATTC
TGAGCCGTGGCGATCCCATCCCACTCCAGCGCCTGGCTTCGCTGCTGACCATGGTGATTTTGACGGTGAACATGTCCAAA
AAGCGCAAATCGTCCCCTATAAAACTGTCGACCTTCACCAAGTACCGACGCAACGTGGCTAAGTCGTTGTACTACGATAT
GTCGTCCAAGACAGTGTTCTTTGAGTACCACTTGAAGAACACTCAGGACCTGCAGGAAGGCCTGGAGCAGGCCATCGCTC
CGTACAACTTCGTAGTGAAGGTGCATAAGAAACCCATAGACTGGCAGAAACAACTTAGTAGCGTCCACGAACGCAAGGCA
GGCCACCGTTCGATCCTGTCCAATAATGTGGGCGCCGAGATTTCCAAGCTGGCAGAGACCAAAGATAGCACTTGGTCGTT
CATCGAACGAACCATGGACCTGATCGAGGCTCGCACCCGTCAGCCCACCACCCGGGTTGCATATCGGTTTCTGCTGCAGC
TGACGTTCATGAACTGTTGCCGTGCGAATGACTTGAAGAACGCCGATCCCAGCACGTTCCAGATCATTGCTGATCCCCAC
CTGGGTCGTATCCTCCGCGCCTTTGTGCCCGAGACAAAGACCAGTATCGAGCGGTTTATCTACTTCTTCCCATGTAAAGG
CCGCTGCGATCCACTCCTTGCCTTGGACAGTTACCTGTTGTGGGTGGGCCCGGTGCCCAAGACGCAGACCACGGATGAAG
AGACGCAATACGACTATCAGCTGTTGCAAGATACACTCCTTATCAGCTACGATCGCTTCATAGCCAAAGAAAGTAAGGAA
AATATCTTCAAGATTCCCAACGGACCGAAGGCTCACCTGGGCCGCCACCTCATGGCCTCGTACCTTGGAAATAATTCGCT
TAAGTCGGAGGCTACGCTGTACGGTAACTGGTCGGTGGAACGGCAAGAGGGAGTTTCGAAAATGGCCGACAGCCGATACA
TGCACACCGTTAAGAAAAGCCCTCCTTCCTACCTCTTCGCCTTTTTGTCGGGTTATTACAAGAAGAGTAACCAAGGCGAA
TACGTGCTTGCAGAAACCCTCTACAACCCCTTGGATTACGATAAAACACTGCCAATAACTACCAATGAGAAGTTGATCTG
TCGCCGGTATGGTAAGAACGCGAAGGTGATCCCCAAAGATGCCCTGTTGTATCTGTACACCTATGCTCAGCAGAAGCGTA
AACAGCTTGCCGATCCGAATGAACAGAATCGCCTGTTTTCGAGCGAATCCCCGGCACACCCCTTCCTGACTCCCCAGTCG
ACGGGCAGCTCGACGCCGCTGACCTGGACCGCACCGAAGACGCTTTCCACCGGCCTGATGACACCGGGCGAAGAGGGATC
CCATGGCTTCCCTCCAGAGGTGGAGGAGCAAGATGATGGCACTCTCCCCATGAGCTGCGCTCAAGAGAGTGGCATGGATC
GTCACCCCGCTGCTTGCGCCTCGGCTCGCATCAACGTGTAATCTAGA

Fig. S1. The DNA sequences encoding recombinases B3, KD, and B2 are shown. The sequences have been codon optimized for *Drosophila*. The coding sequence of the recombinases are shown in black (the initiating ATG codon is underlined); a 7-bp translation initiation sequence (16), shown in blue, was included immediately upstream of the ORF. A C-terminal PEST sequence comprised of residues 422–461 from the mouse ornithine decarboxylase gene (see main text) was inserted as a C-terminal fusion (shown in red). Restriction enzyme recognition sequences used as linkers are shown in green.

R Recombinase

CTCGAGAATCAAAATGCAGCTTACCAAGGACACTGAGATTTCCACTATAAACCGACAGATGTCCGACTTCTCCGAACTGA
GTCAGATTCTCCCCCTGCACCAGATCAGCAAGATTAAGGACATTCTGGAGAACGAGAACCCACTGCCGAAGGAAAAGCTC
GCCAGCCACCTGACTATGATTATTCTTATGGCTAACCTGGCATCGCAAAAGCGTAAAGATGTGCCGGTTAAGCGCTCGAC
ATTCCTTAAGTATCAGAGGTCCATCAGCAAGACGCTCCAATACGATTCCTCGACAAAAACAGTCTCGTTCGAGTACCACC
TTAAGGACCCGAGCAAATTGATCAAGGGCCTTGAGGACGTTGTGAGTCCGTACCGTTTTGTCGTGGGTGTGCATGAGAAG
CCGGACGATGTGATGAGCCATCTTAGCGCCGTACACATGCGTAAGGAGGCAGGCCGCAAGCGTGATCTCGGCAACAAGAT
CAATGACGAGATAACGAAAATCGCGGAGACCCAGGAGACGATCTGGGGATTTGTCGGAAAGACCATGGATCTCATTGAAG
CGCGGACTACACGGCCAACCACAAAAGCTGCCTACAATCTGCTCCTGCAAGCCACTTTCATGAACTGCTGTCGCGCCGAT
GACCTTAAAAACACAGACATCAAGACATTTGAGGTCATTCCGGACAAGCACTTGGGACGGATGCTCCGAGCGTTTGTCCC
GGAGACGAAGACAGGCACCCGCTTTGTGTACTTCTTTCCTTGCAAAGGACGGTGCGATCCGCTGCTGGCTCTGGACAGTT
ACCTGCAGTGGACTGATCCGATCCCTAAAACACGCACCACGGATGAGGATGCCCGCTATGACTACCAACTGTTGCGTAAC
TCGTTGCTGGGTAGCTATGATGGTTTCATTAGTAAGCAGTCCGACGAATCGATATTCAAGATTCCCAATGGTCCGAAGGC
GCACCTGGGTCGCCACGTGACGGCATCCTATTTGAGCAACAATGAGATGGACAAGGAGGCAACATTGTATGGAAACTGGT
CGGCAGCCCGCGAAGAAGGTGTCAGCAGGGTCGCTAAAGCGCGCTACATGCATACCATTGAGAAGTCGCCTCCAAGCTAC
CTTTTTGCTTTTCTGTCCGGATTTTACAACATTACCGCCGAGCGAGCGTGCGAACTGGTGGACCCAAACTCCAACCCCTG
TGAGCAAGACAAGAATATACCAATGATAAGCGATATAGAGACACTTATGGCACGTTACGGAAAGAATGCAGAAATCATCC
CGATGGATGTGCTGGTCTTCTTGAGCTCGTACGCAAGGTTTAAGAACAACGAGGGTAAGGAATATAAGCTGCAAGCTCGG
TCGAGCCGCGGAGTGCCAGATTTTCCAGATAACGGACGAACAGCGCTCTATAACGCCCTGACTGCGGCCCATGTTAAGCG
CAGGAAAATCTCGATAGTCGTAGGACGTTCCATCGACACCTCGGGATCCCATGGCTTCCCTCCAGAGGTGGAGGAGCAAG
ATGATGGCACTCTCCCCATGAGCTGCGCTCAAGAGAGTGGCATGGATCGTCACCCCGCTGCTTGCGCCTCGGCTCGCATC
AACGTGTAATCTAGA

FLP Recombinase

CTCGAGAATCAAAATGCCGCAGTTTGATATCCTCTGCAAGACCCCACCAAAGGTGTTGGTGCGTCAATTCGTGGAGCGAT
TTGAGAGGCCGTCGGGTGAGAAGATCGCCCTGTGCGCTGCCGAGTTGACCTATTTGTGTTGGATGATCACTCATAATGGC
ACCGCGATTAAGCGCGCTACCTTTATGAGCTATAACACTATCATTAGCAATTCCCTGTCCTTTGACATAGTAAACAAGTC
CCTGCAGTTTAAATACAAGACTCAGAAGGCCACTATATTGGAGGCTTCGCTGAAAAAGTTGATCCCGGCATGGGAGTTCA
CGATCATCCCATACTACGGTCAGAAACACCAGAGCGATATTACCGATATTGTAAGCAGCCTCCAGCTGCAGTTTGAGTCC
AGCGAAGAGGCTGATAAGGGTAATAGTCACAGCAAAAAGATGCTGAAGGCACTGCTGTCCGAGGGCGAAAGCATCTGGGA
GATTACTGAGAAAATCCTGAACTCGTTTGAGTACACCAGCCGATTCACCAAGACGAAGACCCTGTACCAGTTCCTCTTTT
TGGCAACCTTCATCAATTGTGGTCGCTTCAGTGACATCAAAAACGTGGACCCTAAATCGTTCAAGCTGGTGCAGAATAAG
TACCTGGGTGTTATCATCCAGTGCTTGGTTACCGAGACTAAGACCTCCGTGTCCAGGCACATTTATTTCTTCTCCGCAAG
GGGTCGCATCGATCCGCTGGTATACTTGGATGAGTTCCTTCGGAATAGTGAACCAGTCTTGAAGCGCGTGAACAGGACGG
GCAATTCCAGTAGCAACAAGCAAGAGTACCAGCTGCTGAAGGATAATCTTGTTCGGTCGTACAACAAAGCCTTGAAGAAA
AATGCGCCATACTCGATCTTTGCAATCAAGAATGGTCCCAAGAGTCATATTGGCCGGCACCTGATGACCAGTTTCTTGTC
CATGAAGGGTCTGACTGAGCTCACAAACGTCGTTGGCAACTGGTCGGACAAGCGAGCGAGTGCCGTCGCCCGCACGACAT
ACACCCACCAGATCACGGCCATACCAGATCACTATTTCGCGCTGGTGTCGCGTTATTATGCCTATGATCCCATCAGCAAG
GAGATGATCGCGCTGAAGGACGAAACCAATCCAATCGAGGAGTGGCAGCATATCGAGCAACTTAAGGGAAGCGCTGAGGG
TAGCATCCGTTACCCCGCCTGGAACGGCATCATCAGCCAGGAGGTTCTGGATTACCTGAGCTCCTACATCAATCGCCGTA
TTGGATCCCATGGCTTCCCTCCAGAGGTGGAGGAGCAAGATGATGGCACTCTCCCCATGAGCTGCGCTCAAGAGAGTGGC
ATGGATCGTCACCCCGCTGCTTGCGCCTCGGCTCGCATCAACGTGTAATCTAGA

Fig. S2. The DNA sequences encoding recombinases R and FLP are shown. The FLP sequence encodes an aspartic acid residue at position 5 (D5). The sequences have been codon optimized for *Drosophila*. Color coding is as in Fig. S1.

A: Blown-OUT stop cassette

AGATCTGGTTGCTTAAGAATAAGTAATTCTTAAGCAACCTAACGTAAGCTAGCTAGACCG
GTGTCGACTAAAGCCAAATAGAAAATTATTCAGTTCCTGGCTTAAGTTTTTAAAAGTGAT
ATTATTTATTTGGTTGTAACCAACCAAAAGAATGTAAATAACTAATACATAATTATGTTA
GTTTTAAGTTAGCAACAAATTGATTTTAGCTATATTAGCTACTTGGTTAATAAATAGAAT
ATATTTATTTAAAGATAATTGCGTTTTTATTGTCAGGGAGTGAGTTTGCTTAAAAACTCG
TTTAGGTTTGTCCTCCCGAAATTATTTATTTAAATGCGATGGAGAGTTGGCGCCGAATCG
AAAACTTTACGCGCTTAAAAGCACGAGTTGGCATCCCTAACGCGTAGGATCTTTGTGAAG
GAACCTTACTTCTGTGGTGTGACATAATTGGACAAACTACCTACAGAGATTTAAAGCTCT
AAGGTAAATATAAAATTTTTAAGTGTATAATGTGTTAAACTACTGATTCTAATTGTTTGT
GTATTTTAGATTCCAACCTATGGAACTGATGAATGGGAGCAGTGGTGGAATGCCTTTAAT
GAGGAAAACCTGTTTTGCTCAGAAGAAATGCCATCTAGTGATGATGAGGCTACTGCTGAC
TCTCAACATTCTACTCCTCCAAAAAAGAAGAGAAAGGTAGAAGACCCCAAGGACTTTCCT
TCAGAATTGCTAAGTTTTTTGAGTCATGCTGTGTTTAGTAATAGAACTCTTGCTTGCTTT
GCTATTTACACCACAAAGGAAAAAGCTGCACTGCTATACAAGAAAATTATGGAAAAATAT
TTGATGTATAGTGCCTTGACTAGAGATCATAATCAGCCATACCACATTTGTAGAGGTTTT
ACTTGCTTTAAAAAACCTCCCACACCTCCCCCTGAACCTGAAACATAAAATGAATGCAAT
TGTTGTTGTTAACTTGTTTATTGCAGCTTATAATGGTTACAAATAAAGCAATAGCATCAC
AAATTTCACAAATAAAGCATTTTTTTCACTGCATTCTAGTTGTGGTTTGTCCAAACTCAT
CAATGTATCTTATCATGTCTGGATCACTAGTGATCTGGCCGGGGTTGCTTAAGAATAAGT
AATTCTTAAGCAACCCTCGAG

B: KD recombination site used in the Kicked-OUT stop cassette
AAACGATATCAGACATTTGTCTGATAATGCTTCATTATCAGACAAATGTCTGATATCGTTT

C: B2 recombination site used in the Baild-OUT stop cassette
GAGTTTCATTAAGGAATAACTAATTCCCTAATGAAACTC

D: RS recombination site used in the Rpd-OUT stop cassette
TTGATGAAAGAATAACGTATTCTTTCATCAA

E: FRT recombination site used in the Flpd-OUT stop cassette
GAAGTTCCTATACTTTCTAGAGAATAGGAACTTC

Fig. S3. Stop cassettes. (*A*) The sequence of the Blown-OUT stop cassette is shown. The stop cassettes used for each recombinase differed only by the sequence of the recombinase target site, shown here for B3 in the green boxes, that flank the transcriptional terminators. Note that recombination sites for B3 and the other recombinases are themselves inverted repeats separated by a spacer that determines the directionality of the recombination reaction. The same tandem transcriptional terminators, which are derived for the *Drosophila* Hsp70Bb gene (ref. 3; shown in blue) and the early SV40 transcription unit (refs. 17 and 18; shown in red) were used in all stop cassettes. The sequence of the target sites used for the other recombinases are shown in *B*–*E*; references for these target site sequences can be found in the main text.